OPEN

Pressure-induced planar N_6 rings in potassium azide

Jie Zhang[1], Zhi Zeng[1,2,3], Hai-Qing Lin[2] & Yan-Ling Li[4]

[1]Key Laboratory of Materials Physics, Institute of Solid State Physics, CAS, and Department of Physics, University of Science and Technology of China, Hefei 230031, China, [2]Beijing Computational Science Research Center, Beijing 100084, China, [3]Kavli Institute for Theoretical Physics China, CAS, Beijing 100190, China, [4]School of Physics and Electronic Engineering, Jiangsu Normal University, Xuzhou 221116, China.

Correspondence and requests for materials should be addressed to Z.Z. (zzeng@theory. issp.ac.cn)

The first-principles method and the evolutionary algorithm are used to identify stable high pressure phases of potassium azide (KN_3). It has been verified that the stable phase with space group $I4/mcm$ below 22 GPa, which is consistent with the experimental result, will transform into the $C2/m$ phase with pressure increasing. These two phases are insulator with N_3^- anions. A metallic phase with $P6/mmm$ symmetry is preferred above 40 GPa, and the N atoms in this structure form six-membered rings which are important for understanding the pressure effect on N_3^- anions and phase transitions of KN_3. Above the studied pressure (100 GPa), a polymerization of N_6 rings may be obtained as the result of the increasing compactness.

M etal azides have drawn considerable attention for their interesting chemical and physical properties. Under external influences (impact, heat, irradiation, etc), they become unstable and decompose into metal and nitrogen[1]. Their practical applications include explosives, pure nitrogen sources and photographic materials. Additionally, metal azides are structurally simple among solids that deflagrate or detonate, so they are potentially model systems for theories of the fast reactions[2]. Being different from the extensively studied alkali halides, metal azides are ionic compounds containing internal molecular structure which makes them the candidates for understanding the complex nature of chemical bonding. On the other hand, the polymerization of nitrogen may form a high-energy-density material because the transformation from the N–N single bond (160 kJ/mol) to the N≡N triple bond (954 kJ/mol) is accompanied by a large energy release. The non-molecular nitrogen under high pressure was first predicted theoretically by A. K. McMahan et al.[3]. A single-bonded cubic gauche form of N_2 (cg-N) was also successfully synthesized by M. I. Eremets et al.[4,5]. It is suggested that cg-N can be stabilized in compounds with other elements or by introducing impurities[4]. Recently, metal azides have been proposed to be a precursor in the formation of polymeric nitrogen. It could be expected that the N_3^- anion will create polymeric single-covalent-bond networks more easily than diatomic nitrogen because the N_3^- anion is more weakly bonded than the diatomic triple-bonded nitrogen[6]. Alkali azides are one class of compound among metal azides. Pressure-induced phase transitions in alkali azides have been reported by both experimental[6-11] and theoretical investigations[12-16]. Previous study reported that sodium azide undergoes a set of phase transitions[6,8], and the N_3^- anions in NaN_3 transform to polymeric nitrogen net above 120 GPa[6]. Lithium azide, which is isostructural to the low-temperature phase of NaN_3 at ambient condition, is stable up to the pressure of 60 GPa at room temperature[7]. Recent high-pressure study of CsN_3 up to 55.4 GPa reveals three phase transitions approximately at 0.5, 4.4, and 15.4 GPa[11]. Strikingly, theoretical studies have predicted polymerization of nitrogen in LiN_3[14,15] and NaN_3[16]. Thus, a study of the high-pressure behavior of KN_3 would provide more insights into the mechanism of pressure-induced rearrangement of azide anions. It is helpful to investigate theoretically the pressure effect on potassium azide which might result in the formation of polymeric nitrogen.

At ambient condition, potassium azide crystallizes in a body-centered tetragonal lattice with $I4/mcm$ symmetry, and the N_3^- ion in the lattice is a straight chain of three nitrogen atoms. Raman scattering up to 4.0 GPa[17] and single-crystal x-ray diffraction up to 7.0 GPa[18] show that no phase transition is found at these measured pressures. Recently, a structural phase transition at 15.5 GPa is revealed by X-ray diffraction study[9,10]. A Raman scattering study of KN_3 up to 55.0 GPa suggests that a first-order phase transition starts at 13.6 GPa and completes at 32.2 GPa[10]. However, a detailed structure of solid KN_3 under high pressure has been unsolved yet. In this paper, we employ the first-principles study to understand the phase transitions and properties of KN_3 under high pressure.

In the present work, KN_3 is compressed up to 100 GPa. The phase transition from $I4/mcm$ to $C2/m$ is determined at a pressure about 22 GPa. In addition, we have defined another high-pressure phase with $P6/mmm$ symmetry in which the N_3^- ions transform to N_6 rings, and the hexagonal phase is metallic. We have just noticed the discussion on the $P6/mmm$ phase by Li et al. recently[19]. The three phases of this crystal are stable against decomposition of KN_3 into $K + \frac{3}{2}N_2$ under pressure up to 100 GPa. The results provide an insight into the formation of polymeric nitrogen in metal azides.

Computational details

To find the lowest energy structures of KN_3 under extreme conditions, the USPEX code based on the evolutionary algorithm[20,21] is employed for the search where the VASP code[22] is used as an external *ab initio* code for the underlying structural optimizations. Evolutionary variable-cell structure prediction simulations are performed at 20, 60, and 100 GPa with 1, 2, and 4 KN_3 formula units per unit cell. The first generation is produced randomly. All newly generated structures are relaxed at constant pressure and ranked by their enthalpy value. The lowest-enthalpy 60% structures of each generation are used to produce the next generation through heredity (70%), atomic permutation (10%), atom position mutation (10%) and lattice mutation (10%). The structures are relaxed by using density-functional theory with the Perdew-Burke-Ernzerhof (PBE) exchange correlation functional[23], and projector augmented wave (PAW) method[24] is also adopted. The $3s^23p^64s^1$ for K and $2s^22p^3$ for N are treated as valence electrons. Having selected the lower enthalpy structures, we recalculate their enthalpies with increased accuracy between 0 and 100 GPa. An energy cutoff of 520 eV is used for the plane-wave basis sets, and the total energy is converged to 1.0×10^{-6} eV in the self-consistent loop. The atomic positions, lattice parameters, and cell volume are fully optimized by using a conjugate-gradient algorithm. The iterative relaxation of the atomic positions stop when all forces are smaller than 0.001 eV/Å, and the total stress tensor is reduced to the order of 0.01 GPa. The phonon calculations are performed using the Quantum ESPRESSO code based on density functional perturbation theory[25], where vanderbilt ultrasoft pseudopotentials are used for K and N. Before the application, the pseudopotentials are tested by comparing the relaxed structural parameters and electronic structure with the results obtained from VASP code. All cases concerned are zero-temperature ground state.

Results and discussion

The analysis of the predicted structures gives us a list of candidate structure with space groups $I4/mcm$, $C2/m$, $P2_1$, $Cmc2_1$, $P6/mmm$, $P\bar{1}$, and $Imma$, which are depicted in Fig. 1. In order to exam the difference between theoretical results and experimental data, the theoretical lattice constants and unit cell volume are compared with experimental $I4/mcm$ structure at ambient condition (Table I). The LDA calculations underestimate a, c, and V by 3.3%, 5.2%, and 11.4%, whereas GGA calculations overestimate a, c, and V by 1.5%, 2.0%, and 5.2%, respectively. The GGA results are closer to the experimental results than the LDA ones. Therefore the GGA exchange-correlation functional is adopted for the further calculations. The $C2/m$ structure detected from the simulations has the same space group as in LiN_3[7], NaN_3[26] and CsN_3[11]. The $I4/mcm$, $C2/m$, $P2_1$ and $Cmc2_1$ structures possess linear molecular N_3^- anions, while the structures with $P\bar{1}$ and $Imma$ symmetries display the characteristic of the N-atom chains and are radically different from the structures containing N_3^- anions (see Fig. 1 and supplementary Table S1). In variable-cell simulations at 100 GPa, the $P6/mmm$ structure is clearly identified as the most stable one and it is assigned to a new structure type for alkali metal azides. Interestingly, this is a layer-like structure with six N atoms forming a planar N_6 ring. Additionally, polynitrogen molecules as clean high energy density
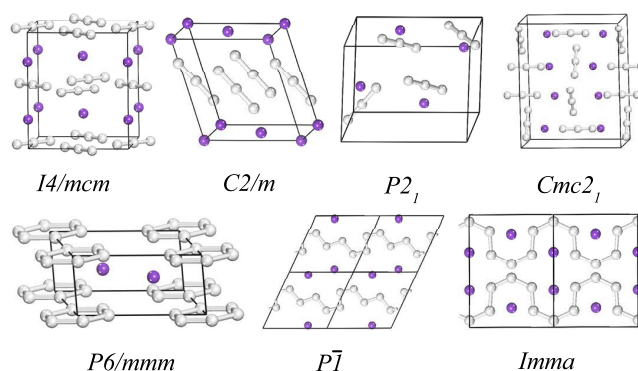
Figure 1 | The structures computed for KN_3 in the pressure range 0–100 GPa. The purple spheres are potassium atoms and grey are nitrogen atoms. The $2 \times 1 \times 2$ supercell of the $P\bar{1}$ structure and the $2 \times 1 \times 1$ supercell of the $Imma$ structure are viewed along b-axis.

materials have been extensively explored for several years[27–29]. A lot of theoretical work on N_6 has shown that the planar hexagonal (D_{6h}) ring is not minimum[30–32]. However, the six-membered nitrogen rings can be stabilized by coordinate covalent to oxygen[33] and by the incorporation of metal atom in metal-N_6 molecules[34]. We now obtain the N_6 rings in bulk materials. It reveals that extra atoms play an important role in stabilizing N_6 ring. More recently, a $P6/m$ structure containing N_6 ring has been also predicted in LiN_3[13–15] and NaN_3[16]. Thus, the $P6/m$ structure is considered in KN_3. The results show that the $P6/m$ structure becomes $P6/mmm$ phase after structure optimization. Parameters describing the $C2/m$ and $P6/mmm$ structures are listed in Table II.

The enthalpies of the most energetically competitive structures are compared over the pressure range 0-100 GPa as shown in Fig. 2. The most stable structure is a tetragonal phase with $I4/mcm$ symmetry from ambient pressure up to 22 GPa, which is then replaced by a lower-enthalpy $C2/m$ structure. Actually, at 13.6 GPa, Raman spectra[10] have identified a phase transition that completes at 32.2 GPa, which is in agreement with the $C2/m$ phase being stable above 22 GPa. The $I4/mcm$-$C2/m$ sequence has also been observed in CsN_3[11]. During $I4/mcm$-$C2/m$ transition, the tetragonal lattice is distorted under pressure, and the orientation of N_3^- anions changes between the two K layers. The N_3^- anion in the $C2/m$ structure is parallel to one another. Moreover, compression induces a symmetry reduction and N_3^- anions are still in a molecular state in this transition, which are consistent with the experimental results[10]. Above 40 GPa, a hexagonal structure with $P6/mmm$ symmetry is favored over other structures and remains the lowest-enthalpy phase up to 100 GPa. We find that the crystal structures of KN_3 containing the N_3^- ions are energetically favorable at lower pressure, while at higher pressure, there is a tendency to the N chains or rings. Although pressure induces the rearrangement of azide ions, the formation of N–N single bond needs further compression. The dependence of volume on pressure is shown in the inset of Fig. 2. The volume reductions of ~2.3% and ~9.5% are found for the $I4/mcm$–$C2/m$

Table I | Theoretical lattice constants and unit cell volumes V at ambient pressure compared with experimental data for $I4/mcm$ structure

Parameter	Experiment (ref. 9)	Present work	
		LDA	GGA
$a = b$(Å)	6.11094	5.90883	6.20556
c(Å)	7.09755	6.72696	7.24091
V(Å^3)	265.043	234.867	278.841

Table II | Optimized structural parameters of $C2/m$ phase at 30 GPa and $P6/mmm$ phase at 100 GPa from the first-principles calculations

Pressure(GPa)	Space group	Lattice parameters(Å,°)	Atomic coordinates(fractional)
30	$C2/m$	$a = 4.293, b = 4.360, c = 4.767$ $\alpha = 90, \beta = 107.969, \gamma = 90$	K 2a (0.0000, 0.0000, 0.0000) N 2d (0.0000, 0.5000, 0.5000) N 4i (0.6272, 0.0000, 0.3151)
100	$P6/mmm$	$a = b = 5.376, c = 2.366$ $\alpha = \beta = 90, \gamma = 120$	K 2d (0.6667, 0.3333, 0.5000) N 6j (0.0000, 0.2396, 0.0000)

and $C2/m$–$P6/mmm$ transitions, respectively. The discontinuous change in volume indicates that the two phase transitions are first order. As the transformation from $C2/m$ to $P6/mmm$ involves the forming of N-N bonds and is reconstructive, there is a large kinetic barrier. In addition, the possibility of decomposition formula of $KN_3 = K + \frac{3}{2} N_2$ is checked by the enthalpies of decomposition, where we consider $Fm\bar{3}m$, $Pnma$, $I4_1/amd$, and $Cmca$ structures for K[35,36] and the cubic gauche ($I2_13$) structure for the N_2[4,37]. It turns out that the enthalpies of $K + \frac{3}{2} N_2$ are much higher than that of KN_3 at the concerned pressure range (>3.2 eV). Thus the KN_3 crystal keeps stable against decomposition over the 0–100 GPa pressure range.

Since the high-pressure $P6/mmm$ phase is novel for alkali metal azides, it is essential to investigate the properties of $P6/mmm$ structure in detail. The ratios of a/a_0 and c/c_0 for the $P6/mmm$ structure seen in Fig. 3a exhibit that the compression is anisotropic with the reduction of lattice parameter a by 13.97% over the pressure studied, while lattice parameter c decreases by 26.73%. This implies that it is more compressive along interlayer direction than intralayer direction for the layer-like $P6/mmm$ phase. The N_6 ring with D_{6h} symmetry possesses benzene-like characteristics. The charge density of N_6 ring in Fig. 3c suggests that each nitrogen atom forms two σ bonds with its two nearest neighbors by overlapping two sp^2 hybrid orbitals,

which is similar to the C-C bonds of C_6H_6. Additionally, for covalent bonds, there is a general trend in that the shorter the bond length, the stronger the bond strength. As shown in Fig. 3b, the N-N bond length of N_6 ring is longer than that of N=N double bond (1.25Å) but shorter than that of N–N single bond (1.45Å). This means that the σ bond of N_6 ring is weaker than the N=N double bond but stronger than the N–N single bond. In general, pressure induces the destabilization of intramolecular bonds. The structure with N_2 and N_6 units has been reported around 60 GPa by first-principles simulations for pure nitrogen[38]. Recently, a diamondoid structure of the polymeric nitrogen is predicted above 263 GPa[39]. These findings also provide a basis for understanding the high-pressure behavior of nitrogen-related materials. As pressure increases, there is a competition among the σ bond, ionic bond, and van der waals. Thus, it is probably fair to say that N_6 rings in $P6/mmm$ phase will transform to polymeric nitrogen networks under further compression.

The ambient-pressure phase $I4/mcm$ is insulating with a calculated band gap of 4.2 eV at 0 GPa (see supplementary Fig. S1), and the $C2/m$ structure is also found to be an insulator with a band gap of 4.1 eV at 30 GPa (see supplementary Fig. S2). On further compression, KN_3 transforms to a metallic state with $P6/mmm$ symmetry at 40 GPa. Besides, the $P\bar{1}$ and $Imma$ structures are metastable above 60 GPa. The $Imma$ structure is metal (see supplementary Fig. S3), and the $P\bar{1}$ structure is a semiconductor with narrow band gap (0.78 eV, see supplementary Fig. S4). Fig. 4 presents the band struc-
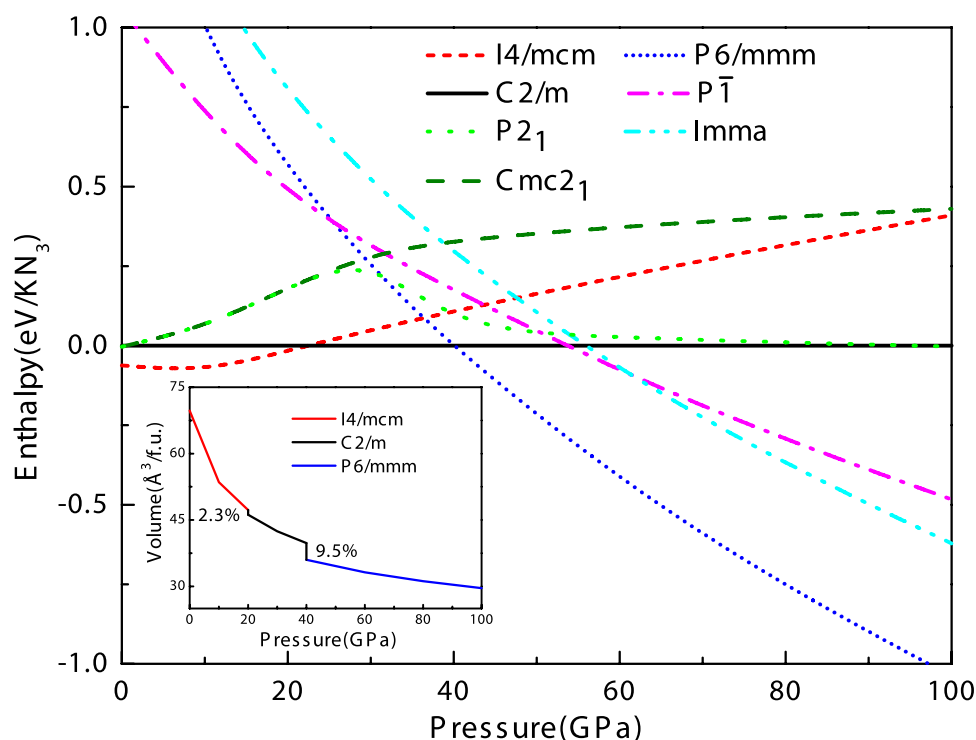

Figure 2 | Calculated enthalpies per KN_3 unit as the function of pressure. The enthalpies are referenced to that of $C2/m$. Inset: the pressure dependence of volume for $I4/mcm$, $C2/m$ and $P6/mmm$ phases of KN_3.
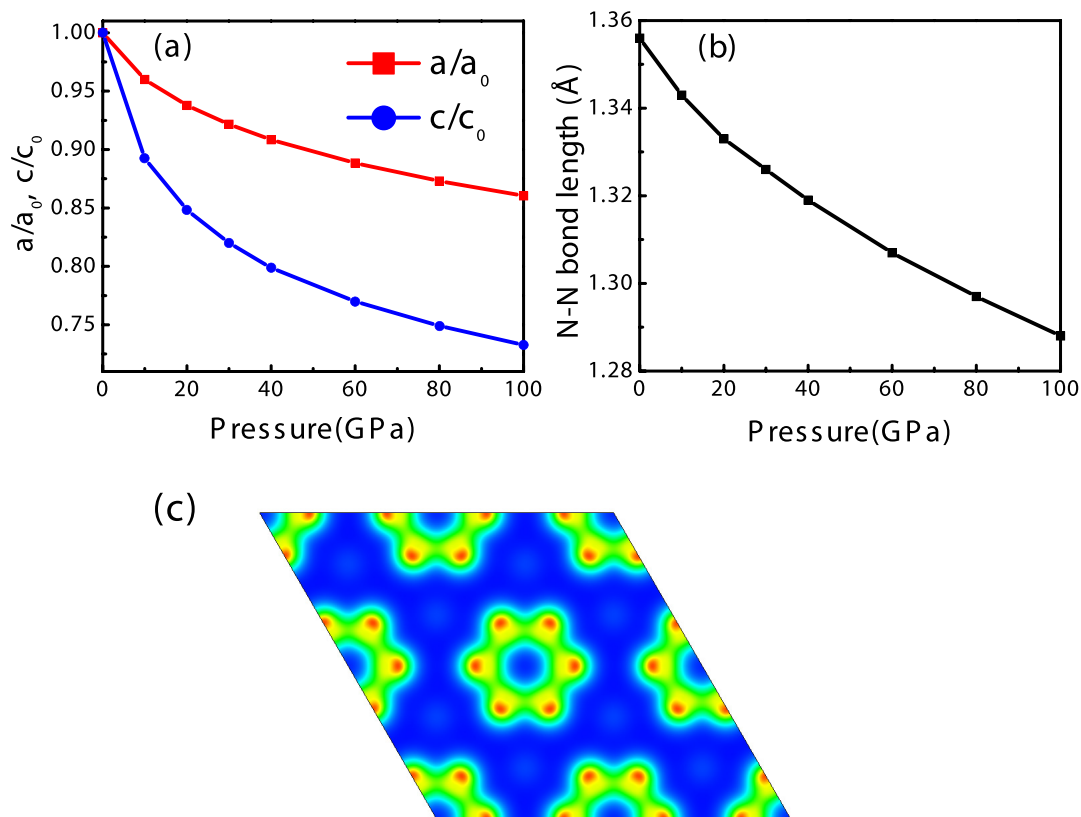
Figure 3 | (a) Variation of normalized lattice parameters of $P6/mmm$ structure with pressure. a_0 and c_0 are the lattice parameters of the equilibrium volume structure at zero pressure. (b) Pressure dependence of the N-N bond length of N_6 ring. (c) Total charge density plotted in the (001) plane for $P6/mmm$ phase at 100 GPa.

ture and the density of states of $P6/mmm$ phase at 100 GPa. It reveals that $P6/mmm$ structure is a weak metal with a small density of states at the Fermi level (0.07 states/eV/cell) which are associated with the N-2p electrons. The bands across the Fermi level are highly dispersive along the c-axis (G → A, H → K, and M → L). In addition, the Bader method[40] is chosen to analyze the charge transfer as implemented in the algorithm developed by Henkelman *et al.*[41]. The Bader charges of the $P6/mmm$ phase are around $+0.73$ and -0.24 for

potassium and nitrogen, respectively, which suggests that the high-pressure $P6/mmm$ phase has ionic characteristics for K-N chemical bonds. It means that the N_6 anion in $P6/mmm$ phase has nearly 8 π-electrons. Six P_z orbitals form three bonding π orbitals and three antibonding π^* orbitals. Thus, the π^* orbitals are partially occupied by two electrons, accompanied by two conduction bands crossing the Fermi level. Furthermore, the dynamical stability of the $P6/mmm$ structure is established from the phonon calculations. As shown in Fig. 5, the absence of any imaginary frequency confirms the stability
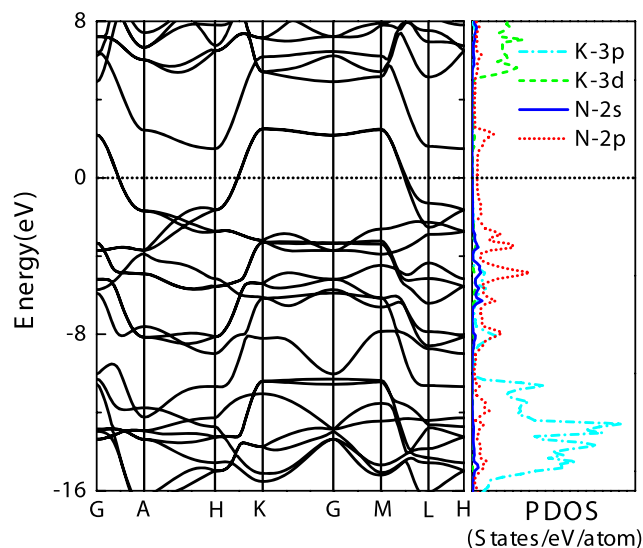
Figure 4 | Electronic band structure and projected density of states (PDOS) for $P6/mmm$ phase at 100 GPa.
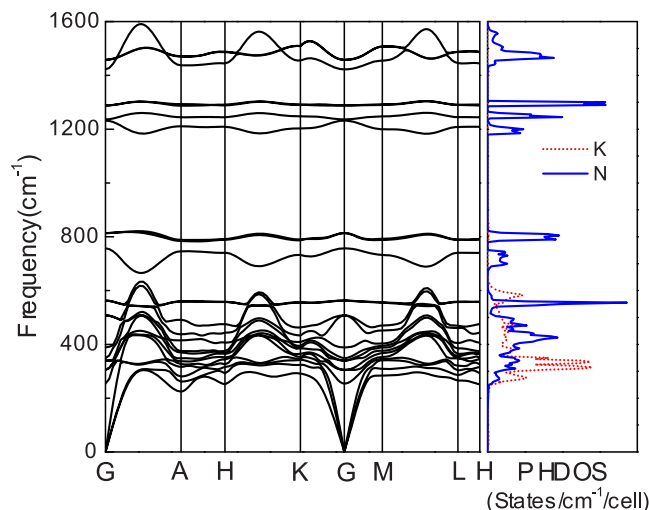
Figure 5 | Phonon dispersion curve and phonon density of states (PHDOS) for $P6/mmm$ phase at 100 GPa.

of the $P6/mmm$ phase. The lower bands, ranging up to 620 cm^{-1}, are formed by a significant mixing of K and N vibrations, while the higher bands are mostly attributed due to N-atom.

Conclusion

In summary, an evolutionary algorithm in conjunction with first-principles electronic structure computations has been used to predict the stable high-pressure phases of potassium azide. Our calculations indicate that the experimental $I4/mcm$ phase of KN$_3$ transforms to $C2/m$ structure at 22 GPa and then to a hexagonal $P6/mmm$ structure at 40 GPa. The planar N$_6$ ring is formed in the metallic $P6/mmm$ phase. This phase of KN$_3$ is dynamically stable. Further compression could lead to the polymerization of N$_6$ rings, which can be used as a potential high-energy-density material.

1. Evans, B. L., Yoffe, A. D. & Gray, P. Physics and chemistry of the inorganic azides. *Chem. Rev.* **59**, 515–568 (1959).
2. Bowden, F. P. & Yoffe, A. D. *Fast Reactions in Solids* (Butterworths Scientific Publications, London, 1958).
3. McMahan, A. K. & LeSar, R. Pressure dissociation of solid nitrogen under 1 Mbar. *Phys. Rev. Lett.* **54**, 1929–1932 (1985).
4. Eremets, M. I., Gavriliuk, A. G., Trojan, I. A., Dzivenko, D. A. & Boehler, R. Single-bonded cubic form of nitrogen. *Nat. Mater.* **3**, 558–563 (2004).
5. Eremets, M. I., Gavriliuk, A. G. & Trojan, I. A. Single-crystalline polymeric nitrogen. *Appl. Phys. Lett.* **90**, 171904 (2007).
6. Eremets, M. I. *et al.* Polymerization of nitrogen in sodium azide. *J. Chem. Phys.* **120**, 10618–10623 (2004).
7. Medvedev, S. A. *et al.* Phase stability of lithium azide at pressures up to 60 GPa. *J. Phys.: Condens. Matter* **21**, 195404 (2009).
8. Zhu, H. *et al.* Pressure-induced series of phase transitions in sodium azide. *J. Appl. Phys.* **113**, 033511 (2013).
9. Ji, C. *et al.* High pressure X-ray diffraction study of potassium azide. *J. Phys. Chem. Solids* **72**, 736–739 (2011).
10. Ji, C. *et al.* Pressure-induced phase transiton in potassium azide up to 55 GPa. *J. Appl. Phys.* **111**, 112613 (2012).
11. Hou, D. *et al.* Series of phase transition in cesium azide under high pressure studied by *in situ* x-ray diffraction. *Phys. Rev. B* **84**, 064127 (2011).
12. Babu, K. R., Lingam, Ch. B., Tewari, S. P. & Vaitheeswaran, G. High-pressure study of lithium azide from density-functional calculations. *J. Phys. Chem. A* **115**, 4521–4529 (2011).
13. Zhang, M., Yan, H., Wei, Q., Wang, H. & Wu, Z. Novel high-pressure phase with pseudo-benzene "N$_6$" molecule of LiN$_3$. *Europhys. Lett.* **101**, 26004 (2013).
14. Prasad, D. L. V. K., Ashcroft, N. W. & Hoffmann, R. Evolving structural diversity and metallicity in compressed lithium azide. *J. Phys. Chem. C* **117**, 20838–20846 (2013).
15. Wang, X. *et al.* Polymerization of nitrogen in lithium azide. *J. Chem. Phys.* **139**, 164710 (2013).
16. Zhang, M. *et al.* Structural and electronic properties of sodium azide at high pressure: A first principles study. *Solid State Commun.* **161**, 13–18 (2013).
17. Christoe, C. W. & Iqbal, Z. Raman scattering in alkali azides at high pressures. *Chem. Phys. Lett.* **39**, 511–514 (1976).
18. Weir, C. E., Block, S. & Piermarini, G. J. Compressibility of inorganic azides. *J. Chem. Phys.* **53**, 4265–4269 (1970).
19. Li, J. *et al.* Pressure-induced polymerization of nitrogen in potassium azides. *Europhys. Lett.* **104**, 16005 (2013).
20. Oganov, A. R. & Glass, C. W. Crystal structure prediction using *ab initio* evolutionary techniques: Principles and applications. *J. Chem. Phys.* **124**, 244704 (2006).
21. Glass, C. W., Oganov, A. R. & Hansen, N. USPEX–Evolutionary crystal structure prediction. *Comp. Phys. Comm.* **175**, 713–720 (2006).
22. Kresse, G. & Furthmüller, J. Efficient iterative schemes for *ab initio* total-energy calculations using a plane-wave basis set. *Phys. Rev. B* **54**, 11169–11186 (1996).
23. Perdew, J. P., Burke, K. & Ernzerhof, M. Generalized gradient approximation made simple. *Phys. Rev. Lett.* **77**, 3865–3868 (1996).
24. Kresse, G. & Joubert, D. From ultrasoft pseudopotentials to the projector augmented-wave method. *Phys. Rev. B* **59**, 1758–1775 (1999).
25. Baroni, S., Gironcoli, S. d., Corso, A. D. & Giannozzi, P. Phonons and related crystal properties from density-functional perturbation theory. *Rev. Mod. Phys.* **73**, 515–562 (2001).
26. Iqbal, Z. Temperature dependence of ramanactive phonons and nature of the phase transition in lithium and sodium azide. *J. Chem. Phys.* **59**, 1769–1774 (1973).
27. Cacace, F., de Petris, G. & Troiani, A. Experimental detection of tetranitrogen. *Science* **295**, 480–481 (2002).
28. Vij, A. *et al.* Polynitrogen Chemistry. Synthesis, chatacterization, and crystal structure of surprisingly stable fluoroantimonate salts of N$_5^+$. *J. Am. Chem. Soc.* **123**, 6308–6313 (2001).
29. Saxe, P. & Schaefer, H. F. Cyclic D$_{6h}$ hexaazabenzeneA relative minimum on the N$_6$ potential energy hypersurface? *J. Am. Chem. Soc.* **105**, 1760–1764 (1983).
30. Glukhovtsev, M. N. & Schleyer, P. v. R. Structures, bonding and energies of N$_6$ isomers. *Chem. Phys. Lett.* **198**, 547–554 (1992).
31. Tobita, M. & Bartlett, R. J. Structures and stability of N$_6$ isomers and their spectroscopic characteristics. *J. Phys. Chem. A* **105**, 4107–4113 (2001).
32. Raczyńska, E. D. On the basicity and π-electron delocalization of 'hexaazabenzene' N$_6$ - Quantum-chemical studies. *Comp. Theor. Chem.* **971**, 38–41 (2011).
33. Wilson, K. J., Perera, S. A., Bartlett, R. J. & Watts, J. D. Stabilization of the pseudo-benzene N$_6$ ring with oxygen. *J. Phys. Chem. A* **105**, 7693–7699 (2001).
34. Duan, H.-X. & Li, Q.-S. A series of novel aromatic compounds with a planar N$_6$ ring. *Chem. Phys. Lett.* **432**, 331–335 (2006).
35. Ma, Y., Oganov, A. R. & Xie, Y. High-pressure structures of lithium, potassium, and rubidium predicted by an *ab initio* evolutionary algorithm. *Phys. Rev. B* **78**, 014102 (2008).
36. Marqués, M. *et al.* Potassium under pressure: A pseudobinary ionic compound. *Phys. Rev. Lett.* **103**, 115501 (2009).
37. Kotakoski, J. & Albe, K. First-principles calculations on solid nitrogen: A comparative study of high-pressure phases. *Phys. Rev. B* **77**, 144109 (2008).
38. Mattson, W. D., Sanchez-Portal, D., Chiesa, S. & Martin, R. M. Prediction of new phases of nitrogen at high pressure from first-principles simulations. *Phys. Rev. Lett.* **93**, 125501 (2004).
39. Wang, X. *et al.* Cagelike diamondoid nitrogen at high pressures. *Phys. Rev. Lett.* **109**, 175502 (2012).
40. Bader, R. F. W. *Atoms in Molecules: A Quantum Theory* (Oxford University Press, New York, 1990).
41. Henkelman, G., Arnaldsson, A. & Jónsson, H. A fast and robust algorithm for Bader decomposition of charge density. *Comput. Mater. Sci.* **36**, 354–360 (2006).

Acknowledgments

Author contributions

J.Z. and Z.Z. conceived the research. J.Z. carried out the calculations. J.Z., Z.Z., H.-Q.L. and Y.-L.L. analyzed the data. J.Z. and Z.Z. wrote the paper.

Additional information